

# Aerodynamics of Formula SAE Racing Cars Conceived Using Computational Fluid Dynamics

**Punith Doddegowda, Aleksandr L.  
Bychkovsky and Albert R. George**

Sibley School of Aerospace and Mechanical Engineering, Cornell University

## ABSTRACT

For many racing teams the use of Computational Fluid Dynamics (CFD) as a design tool could mean a very expensive investment. CFD analysis of the complex separated flows associated with a race car would typically require extensive resources. Through the design of aerodynamics for a Formula SAE race car, this paper illustrates the use of less extensive CFD along with the wind tunnel as a tool that reduces design time. Various meshing techniques are analyzed that do not require extensive computational resources and are fairly simple to implement.

The results obtained from these methods are compared to experimental results from wind tunnel tests. For the design of wings the results show that the coefficient of lift can be predicted fairly accurately to within 10% of the experimental value, but the coefficient of drag is not predicted very well. It is also shown that the design of an effective aerodynamics package can be accomplished with these fairly simple techniques. The improvements in lap times, recorded during testing on a FSAE type race track are presented. A simple and quick manufacturing technique is also analyzed for manufacturing wings using composites like fiberglass and carbon fiber.

## 1. INTRODUCTION – AERODYNAMIC DESIGN

Aerodynamic design of a Formula SAE car is a challenging exercise since the speeds involved are very low when compared to many other forms of open wheel racing. The low speed tracks (top speed of ~62mph [100km/hr] and average speed of ~34mph [55km/hr]) encountered at Formula SAE competitions severely constrains the opportunity for effective aerodynamic improvements. Thus the design goal is to obtain high downforce at relatively low speeds using a combination of various aerodynamic elements. Wings are the most general and popular way of producing downforce along with some use of underbody aerodynamics. Wing

designs range from single element to multi-element. The wing itself can be a single plane or a bi-plane wing. The aerodynamics package can be a combination of front wing, center wing, rear wing and an underbody. Depending on the requirements of the race car these aerodynamic elements can be used separately or in conjunction to provide better traction and cornering ability. There are many options available;

hence a fundamental approach to designing race car aerodynamics without the use of extensive computational or experimental resources is presented in the subsequent sections.

The function of the wing in a race car is to produce downforce while keeping the drag to a minimum. The amount of downforce generated by a specific wing design depends on various factors that include wing profile, operational angle of attack, number of elements and flow separation. While designing for the FSAE car the present approach was to evaluate many design possibilities and select the best according to the requirements of the team. Computational Fluid Dynamics (CFD) was used for the purpose of conducting a quick evaluation of these possibilities.

The commercial CFD code Fluent was used. Meshing was carried out on a computer equipped with 1.5GHz processing capacity and 1GB RAM. 3D calculations were performed on a Windows based cluster with a maximum of 64 processors while 2D calculations were performed using 3-4 similar computers working in parallel.

## 2. VALIDATION OF FLUENT USING A SINGLE ELEMENT WING

The first step prior to use in design was to validate the use of Fluent for the purpose of airfoil design. Hence a single element standard NACA 4415 profile was initially used to investigate the meshing requirements, mesh convergence and the use of various turbulence models available in Fluent. This profile was chosen since there

is extensive experimental data in the literature with which the CFD results could be compared.

The first meshing scheme tried was a structured tetrahedral mesh. With this method a very fine control of the boundary layer can be achieved. A diagram showing this particular scheme is presented in Figure 1. The wall  $Y^+$  values obtained with this can be as low as 1, but it was noticed at this point that the cell aspect ratio was high. For the purpose of our design a wall  $Y^+$  value of around 5 was considered acceptable.

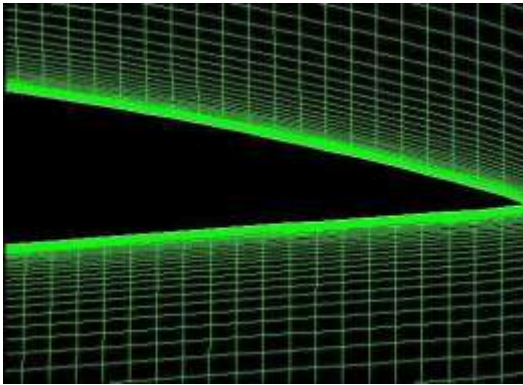


Figure 1: Structured mesh for single element NACA profile with a highly refined Boundary Layer

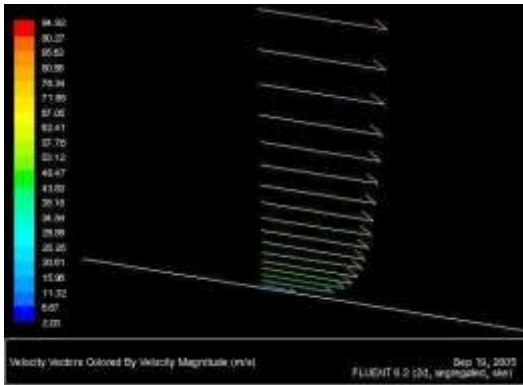


Figure 2: Velocity profile on the suction side of the wing

It was then realized that a structured meshing scheme cannot be successfully used for multi-element wings, thus there was a shift towards unstructured meshes coupled with a boundary layer (BL) mesh so that the BL was still refined to produce accurate results. Structured and unstructured meshes are shown in Figures 3 and 4 respectively.

This scheme is easily adaptable to multi-element wing design. As shown by Lewis and Postle [1] variations of this method can be effectively used depending on what stage of design we are at and the level of accuracy required.

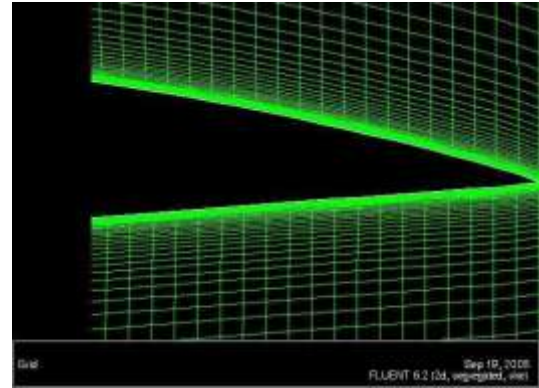


Figure 3: Trailing edge of the wing showing BL resolution for structured mesh

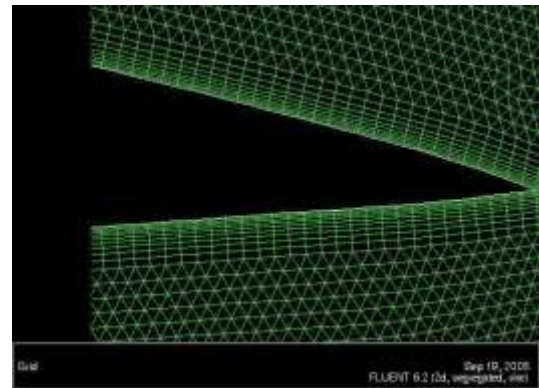


Figure 4: Trailing edge of the wing showing BL resolution for unstructured mesh

When using this method, testing for mesh convergence is of great importance. The unstructured mesh was progressively refined and the change in values of the lift coefficient and drag coefficient were monitored. If the change in these values was less than 1% then it was concluded that mesh convergence was attained.

The  $k-\epsilon$ , Spallart Almaras and Reynolds Stress turbulence models were then each used for CFD calculation of lift and drag. The results were compared to those obtained experimentally in a NASA wind tunnel. These experimental values were obtained from results presented by Abbott and Doenhoff [2]. The comparisons are shown below.

From Figure 5 it can be seen that none of the models are able to predict accurately the stall angle and behavior. Post-stall predictions also vary significantly from the experimental results, which is to be expected due to the difficulties in

accurately computing separation. The coefficient of lift values are close to the experimental values but the coefficient of drag is very different. Figure 6 shows the coefficient of drag calculated from the different models. The values are between 2–3 times the experimental values.

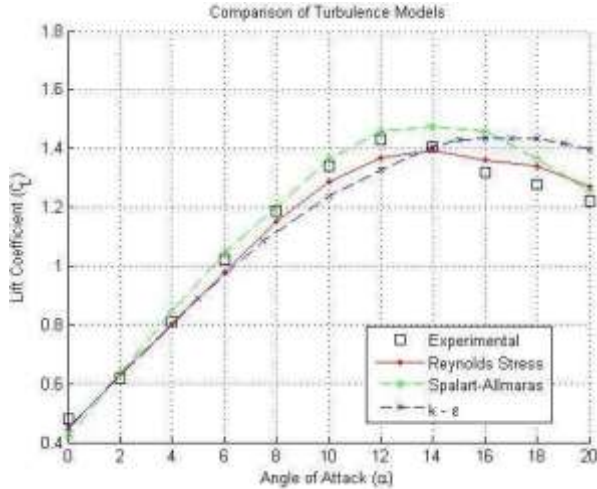


Figure 5: CFD calculation for coefficient of lift with various turbulence models compared to experimental results

The RSM model is more accurate but it is expensive in terms of resources. The Spalart-Allmaras and  $k-\epsilon$  models, which are two equation models, require lesser computational time. The  $k-\epsilon$  model was found to be the most stable. These trends in results agree with the findings of Lewis and Postle [1], who did their calculations for a two-element wing (NLR 3701). This validation process gave us valuable insight into the meshing and turbulence modeling requirements.



the BL meshes. An alternative method is to reduce the BL mesh thickness so that there is no overlap.

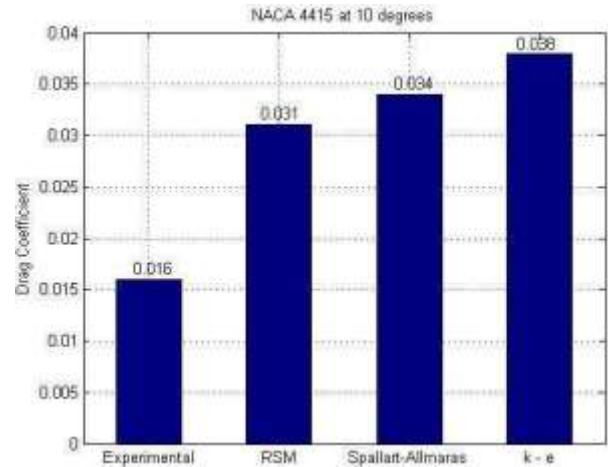


Figure 6: Coefficient of drag obtained from CFD compared to experimental values

As the next step in the design process, analyses of two, three and four element wings were carried out using similar meshing techniques. Katz [3] states that increasing the number of elements delays flow separation and increases the lift that is obtained. Hence the investigation of multi-element wings was crucial to find an optimum design that satisfied team requirements. Three possibilities were considered. A front wing, center wing and rear wing. While the front and rear wings are often seen in formula style racing the center wing or sprint car type wing is unusual for formula cars.

One of the design alternatives considered was a sprint car type wing. This wing is mounted at the center of the car above the driver. CFD calculations were performed for a sprint car wing design that would be center mounted. Figure 7 shows a 2D calculation for this particular design.

Figure 7: 2-D CFD calculation for the Cornell FSAE car with skateboard wing

The main advantage seen in this design was large amounts of downforce that could be generated at the center of the car. The sprint car wing not only produced high downforce but also high drag which is detrimental to acceleration. There are two penalties that the designer is confronted with in using multi-element wings for racing cars, drag and weight.

### 3. MULTI-ELEMENT WING DESIGN

After validation, the process of design was undertaken. The meshing scheme described previously for an unstructured mesh was carefully adapted for multi-element design. When this method is adapted to multi-element wings the gap between the elements is a very critical region and has to be treated carefully. Lewis and Postle [1] suggested the use of a partial BL mesh if the gap size is close to causing overlaps of

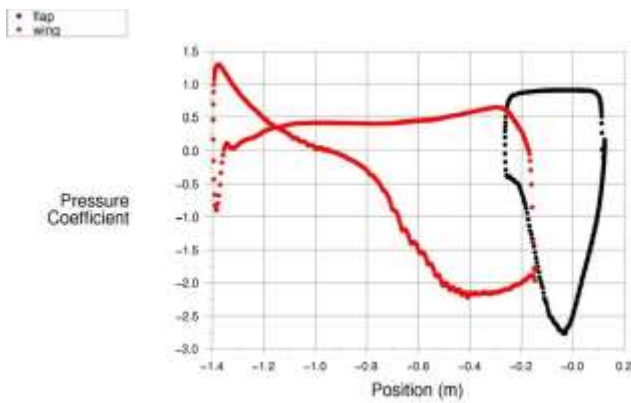


Figure 8: Graph of  $C_p$  along the two element wing

Keeping these in mind, a 4-element (front and rear wing) design was chosen to be within the acceptable weight and drag penalties while producing high lift coefficients. The main plane in this four element design was chosen after calculations were performed on various standard NACA profiles as well as modified NACA profiles. The pressure profile of the main element was then suitably modified by adding a slat and two flaps.

The next step was to conduct extensive CFD analysis of this 4-element design. For this purpose a 3D model was created using Gambit and CFD calculations were performed using the  $k-\epsilon$  turbulence model. The face mesh consisted of a BL mesh attached to the wing and the remaining cells in the inner region were triangular cells. The outer region again consisted of quadrilateral cells. This face mesh was mirrored along the span of the wing resulting in a hexahedral BL, tetrahedral inner region and hexahedral outer region. Figure 9 shows the 3D mesh generated for the four-element wing. CFD calculations were performed for this using the  $k-\epsilon$  model with air speed set at 35Mph.

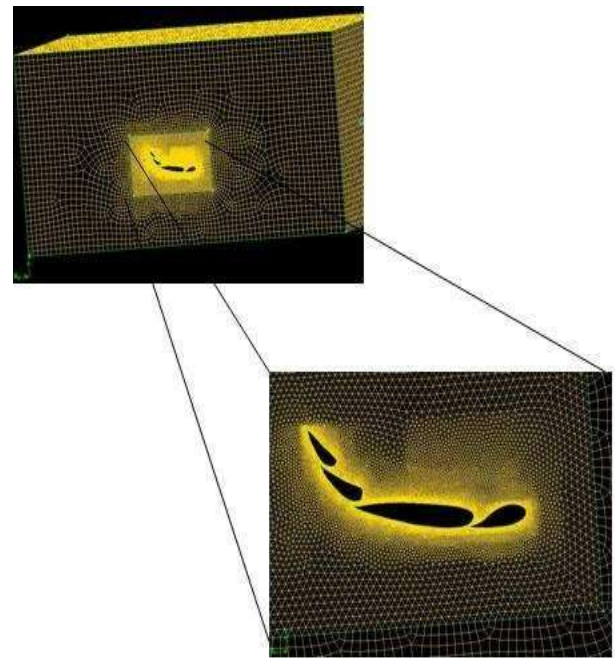


Figure 9: 3D mesh for the four element wing

The CFD results obtained from this model are shown below in Figures 10 and 11. The lift-drag polar, which can be used to find an ideal operating point for the wing, can be seen in Figure 11.

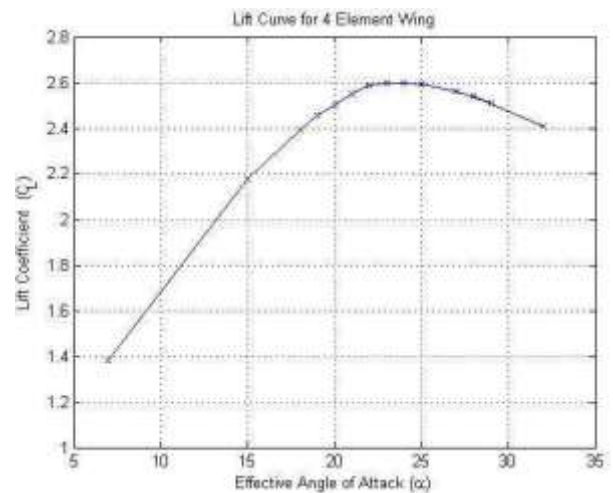


Figure 10: Lift coefficient at various angles of attack obtained from CFD calculations



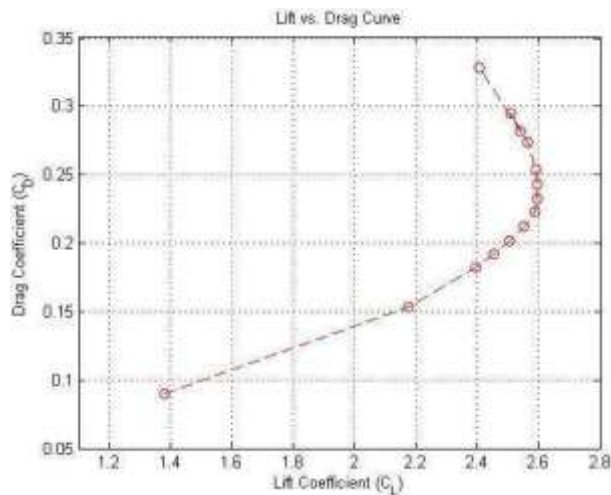


Figure 11: Lift coefficient plotted with drag coefficient at various angles of attack

No aerodynamic design is complete without validating it in the wind tunnel. Hence the next step was to validate the CFD predictions for the four-element wing in a wind tunnel. A 50% model was constructed out of fiberglass composite material. This model was mounted on a force measuring load cell as shown in Figure 12. Lift and drag forces were measured using this instrument. The model of the helmet shown on the right bottom corner was used to study the effect of a helmet on the rear wing. This effect is analyzed in detail in Section 5.

The force measuring device is a multi axis load cell which obtains force and moments in the x, y and z axis. Drag and Lift were measured using this data. The 4x4 wind tunnel at Cornell University was used for this purpose. The tunnel is capable of wind speeds of 70Mph, however all experiments with the model were conducted at 35Mph to stay within the measurement range of the load cell. The effective angle of attack of the four-element wing for these experiments was set at 22 degrees.

The experimental results obtained from the wind tunnel were then compared with the CFD data. Figure 14 shows the comparison between CFD and experimental results. This comparison is for an effective angle of attack of 22 degrees and wind speed of 35Mph. The coefficient of lift is within 10% of the value predicted by CFD, while the coefficient of drag does not compare very well. Some of the reasons for this deviation in predicted drag values could be as follows. Transition occurs into the turbulence regime close to the leading edge. But, there is an initial laminar boundary layer that develops at the leading edge which transforms into a turbulent BL. However the CFD code may predict the transition incorrectly, as compared to the wind tunnel model resulting in a higher skin friction value. Another reason is the over estimation of turbulent viscosity due to numerical dissipation in the code resulting in higher skin friction. Hence while the prediction of the lift coefficient is good, the skin friction is not predicted well.

Figure 12: 50% model of the four-element wing in the windtunnel. (Insert shows “helmet” model.)

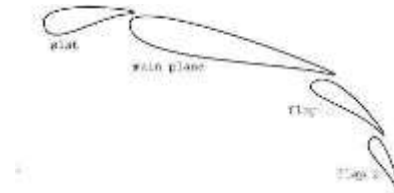


Figure 13: Four-element wing profile showing the slat, mainelement and two flaps

The four-element wing, which has been analyzed, was a basic design that was evolved into the front wing and rear wing depending on the requirements of car balance and handling. These designs are presented in subsequent sections.

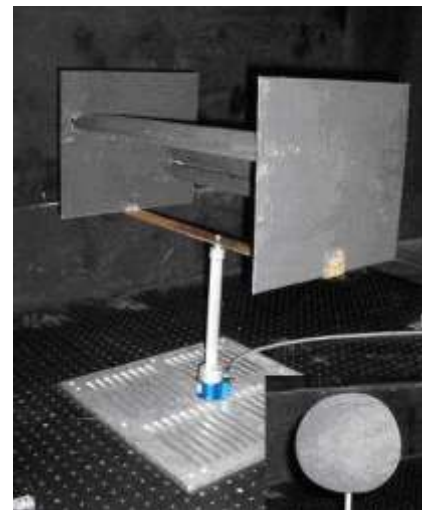
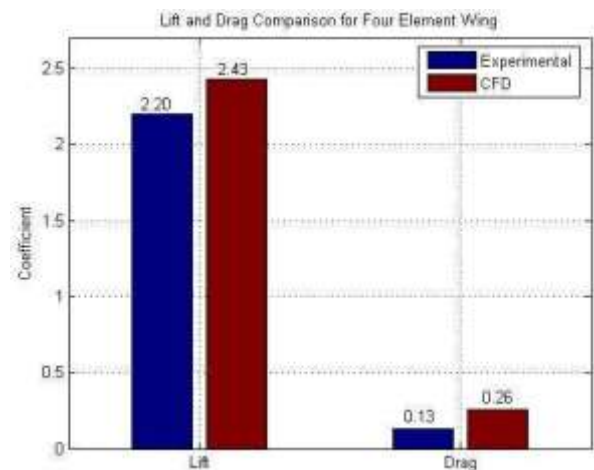


Figure 14: Comparison between results obtained from the wind tunnel and CFD calculation

#### 4. DESIGN OF FRONT WING

The position of the front wing is constrained by the rules of the Formula SAE competition. Any part of the front wing cannot be more than 45.75 cm beyond the plane of the front tires. This throws up a design challenge of producing high lift within the constraints. The wing area is limited, since we did not want to get close to the high-pressure regions formed due to stagnation in front of the front tires. These high-pressure regions increase the adverse pressure gradient on the suction side of the wing. Since, the design was limited in area it was decided to use a high camber overall profile which could produce more lift. High camber profiles are prone to boundary layer separation at lower angles of attack, thus boundary layer control via multiple elements was used.

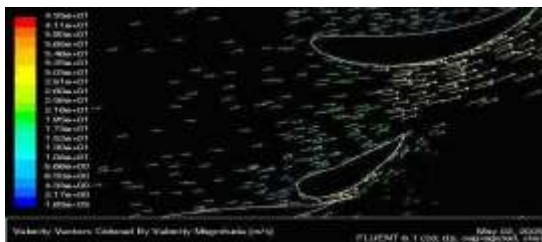


Figure 15: Front wing design showing the first three elements blowing into the high camber element

As shown in Figure 15, the first three elements were set at an angle such that they would blow tangentially into the high camber wing on the suction side in the region where separation was predicted to occur if the high camber wing functioned alone. As suggested in [4] this increases the kinetic energy of the flow on the suction side of the high camber element thus preventing separation while maintaining a high lift coefficient.

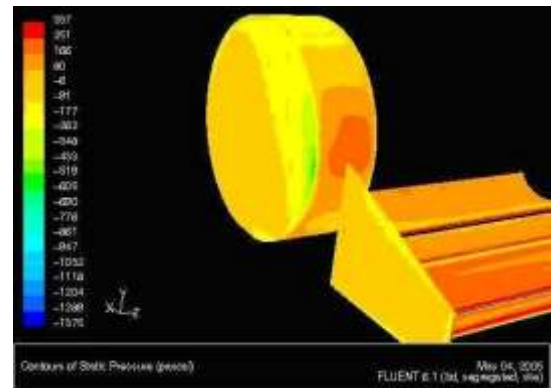


Figure 16: Pressure contours for the front wing in the vicinity of the tire

#### 5. DESIGN OF REAR WING

For the relatively low speed courses seen in FSAE competitions, a rear wing needs to have a high lift coefficient. The drag associated with a high lift device was considered, but it was not one of the major factors of importance because the race car is not power limited at low speeds. Significant improvements of lap times were seen when a coefficient of lift was added to a lap-time simulation program developed by Cornell Racing. However, the coefficient of drag showed very little effect due to which drag was not considered important for the design of FSAE aerodynamics. Furthermore, track test data showed a considerable improvement in lap times with wings on the car in spite of relatively large drag. (See the Performance/Validation section below.).

The major concern and difficulty in rear wing design is getting enough undisturbed, free stream flow to the rear wing. This presents a problem, since the distance between the driver's helmet and the leading edge of the rear wing was well under two chord lengths (restricted by rules on placement of rear wing). To overcome this the wing would need to be mounted at least one-half diameter of the helmet above the plane of the helmet to prevent a loss of more than 10% downforce, as shown by the wind tunnel tests summarized in Figure [17] and Table [1] below.

Moreover, given a fixed horizontal gap between the wing and the helmet (in this case 1–2 helmet diameters away), the vertical gap size should be at least one helmet diameter for

vanishingly small wake effect and hence negligible loss of downforce.

Structural issues and weight transfer / tire performance aspects become involved when placing a wing high above the car; however, for the purpose of this paper we will consider only the aerodynamic effects. In our on car testing no adverse effects were conclusively attributed to adding mass (of rear wing) above the rear bay area.

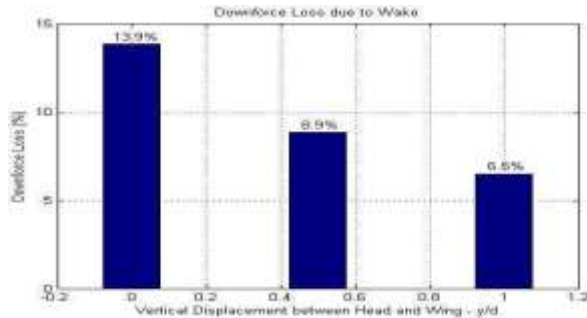


Figure 17: Helmet Effect on 50% Model

Case	Y-gap (y/d)*	X-gap (x/d)*	Loss (%)
centered	0	1.667	13.9
tangent	0.5	1.667	8.9
Below	1	1.667	6.5

\*helmet diameter d [50%] = 0.1524m (6in)

\*\*wing chord c [50%] = 0.275m (10.8in)

Table 1: Helmet/Wake Effect on 50% Scale Model of a FourElement Wing in Wind Tunnel

In order to attain a higher downforce value, without the benefit of ground effects, an extra plane was added to the rear wing to make a bi-plane eight (8) element wing using modified NACA airfoils [6]. The two planes were identical to one another and were spaced 0.92 helmet diameters (or 0.83c) apart. As a result, the top plane of the eight-element wing, positioned 1.92d above the helmet, and thus was mostly clear from the influence of the wake generated by the helmet.

The use of the bi-plane multi-element rear wing showed a significant improvement in lap times. The next natural step was to model the full race car to analyze the interaction of the body and wings. Given the limited meshing resources this has proved to be an arduous task. A CFD calculation performed on a simplified model of the race car is shown in Figure 18.

Figure 19: Track testing with front and rear prototype wings on the race car

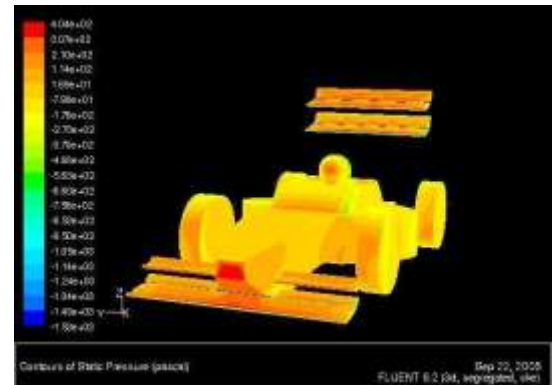


Figure 18: Static pressure contours of a simplified full car model

## CONCLUSION

Computational Fluid Dynamics can be used for the development of an aerodynamics package for a race car even with limited computing resources. Simple CFD evaluations provide the initial base from which promising designs can be picked and evaluated in the wind tunnel. The main conclusions drawn from this paper are as follows.

1. Fairly accurate 2D and 3D CFD evaluations can be performed by race teams for aerodynamics thus accelerating the design cycle by supporting wind tunnel tests.
2. The prediction of coefficient of lift for airfoil design was found to be within 10% of the experimental value, but the coefficient of drag was not predicted very well.
3. The accuracy of CFD calculations depends on mesh refinement and hence more extensive computing resources can lead to better results.

## ACKNOWLEDGEMENTS

The computational work performed could not have been accomplished without computing resources and readily available staff of Cornell University Theory Center.

Some results from this study were presented at the Fluent European Automotive CFD Conference in June 2005.

Validation of computational results through on car testing was made possible with the help of many Cornell Racing (2004–05) team members and their advisor, who were always ready to assist.

## REFERENCES

1. R. Lewis, P. Postle, *CFD Validation for External Aerodynamics*, European Automotive CFD Conference, 2003.
2. I. H. Abbott, A. E. Von Doenhoff, *Theory of Wing Sections*, Dover Publications Inc. (1959)
3. J. Katz, *Race Car Aerodynamics: Designing For Speed* (1995)
4. H. Schlichting, K. Gerten: *Boundary Layer Theory*, Springer Publication (2000)
5. P. G. Wright, *Ferrari Formula 1: Under the Skin of the Championship – Winning F1-2000*, SAE (2004)
6. N. J. McKay, A. Gopalathnam: *The Effects of Wing Aerodynamics on Race Vehicle Performance*, SAE Motorsports Engineering Conference & Exhibition, December 2002, SAE Publication P-382.